# Experimental bond behavior of hybrid rods for concrete reinforcement

Antonio Nanni† and Jeremy S. Nenninger‡

*Department of Architectural Engineering,
The Pennsylvania State University, University Park, PA, 16802, U.S.A.*

Kenneth D. Ash‡†

*BSW, Tulsa, OK, 74103, U.S.A.*

Judy Liu‡‡

*Department of Architectural Engineering,
The Pennsylvania State University, PA 16802, U.S.A.*

**Abstract.** Fiber reinforced plastic (FRP) rods provide certain benefits over steel as concrete reinforcement, such as corrosion resistance, magnetic and electrical insulation, light weight, and high strength. FRP composites can be combined with a steel core to form hybrid reinforcing rods that take advantage of properties of both materials. The objective of this study was to characterize the bond behavior of hybrid FRP rods made with braided epoxy-impregnated aramid or poly-vinyl alcohol FRP skins. Eleven rod types were tested using two concrete strengths. Specific topics examined were bond strength, slip, and type of failure in concentric pull-out tests from concrete cubes. From analysis of identical pull-out tests on both hybrid and steel rods, information on relative bond strength and behavior were obtained. It is concluded that strength is similar but slip in hybrid rods is much higher. Hybrid rods failed either by pull-out or splitting the concrete block (with or without yielding of the steel core). Experimental data showed consistency with similar test results presented in the literature.

**Key words:** bond; braiding; concrete; fiber reinforced plastic (FRP); hybrid reinforcement; pull-out; slip; testing.

## 1. Introduction

Fiber-reinforced plastic (FRP) composites may replace steel reinforcing bars and tendons in some reinforced and prestressed concrete (RC and PC) applications. With their corrosion resistant, electrically and magnetically insulating, high strength, and light weight properties, FRP rods present certain advantages over steel. There are also some notable disadvantages in FRP rods,

---

† Professor
‡ Research Assistant
‡† Project Coordinator
‡‡ Research Assistant

such as a low modulus of elasticity (that may result in excessive deflections of the structural member) and linear-elastic behavior up to failure (that may result in lack of ductility of the structural member). There are many types of FRP composites, varying with constituents, properties and manufacturing. These materials begin with the fibers (usually glass, aramid, or carbon) impregnated with thermoset resins to produce rods, ropes, or fabrics. In the case of hybrid rods, an FRP skin is braided over a steel core to take advantage of the properties of both materials, that is: the FRP provides corrosion protection and tensile strength, whereas the steel provides stiffness and ductility. Among the topics that need to be studied is bond behavior with concrete. The bond behavior of reinforcing rods is important as it affects the strength of any structural RC member, its mode of failure, and the requirement on concrete cover.

The purpose of this study was to perform experimental and analytical work on the pull-out performance of hybrid FRP reinforcing rods and to determine bond behavior in terms of strength, slip, and type of failure. Bond modeling and design considerations are reported elsewhere (Nanni and Liu 1997). In addition to the quantification of bond strength (for comparison with steel reinforcement), the significance of the study is in providing physical evidence of the bond mechanism for hybrid rods during concentric pull-out. Two limitations of this research project are the size of the sample- 39 specimens- and the testing procedure itself. Other types of tests may be more representative of field situations ("Bond" 1982) and may be necessary for the validation of design parameters.

## 2. Background

### 2.1. Types of FRP composites

Common fiber types used in FRP rods are glass, aramid, and carbon. Glass fibers, usually E-glass, are competitive in price, easy to manufacture, and high in strength. The first type of fibers used in such applications, E-glass fibers have tensile strength up to 4500 MPa. Aramid fibers are organic, with tensile strength up to 3100 MPa. Carbon fibers upstage glass and aramid fibers with tensile strength up to 5500 MPa, tensile modulus up to 380 GPa, high compressive strength, immunity from stress corrosion and stress rupture at room temperature, and the ability to maintain strength at high temperatures. These strong fibers are impregnated with thermoset
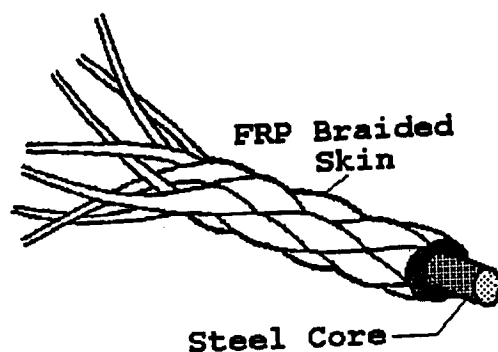


Fig. 1 Hybrid rod.

resins, usually epoxy or vinyl ester, to produce the FRP shapes. The fiber type and volume percentage affect elastic modulus and strength of the composite. Physico-mechanical properties of resins vary widely. Resins hold the fibers together, allow load transfer between fibers, and protect the fibers from the environment. Various shapes and patterns can be achieved by changing the manufacturing parameters: production of FRP reinforcement for concrete is generally done by pultrusion, braiding, filament winding, or their combinations.

### 2.2. Hybrid rods

In the hybrid rods used for this project, epoxy-impregnated yarns are braided and fully bonded to a steel core (see Fig. 1). In this simple composition, there are several possible combinations with various steel to FRP area ratios, grades of core material, and types of fibers. This spectrum of combinations corresponds to a wide range of performance characteristics. At one extreme, the steel core can be used simply to add ductility to the FRP, that is: change the stress-strain diagram from one straight line to two lines, of which the second has a lower rigidity. At the other extreme, the steel can carry a significant percentage of the load with the FRP mainly for corrosion protection (Nanni, *et al.* 1992). Tests were conducted at the Pennsylvania State University on the tensile properties of these rods, as well as on the flexural properties of beams reinforced with hybrid rods of aramid and poly-vinyl alcohol (PVA) fibers. It was found that the FRP skin worked to increase the tensile capacity of the rods, while the steel improved rigidity in the elastic range and prevented the total collapse after the FRP failed. The hybrid rods had a tensile behavior that could be predicted according to the law of mixture (Nanni, *et al.* 1994). Further tests showed that beams reinforced with hybrid rods had a higher ultimate capacity than the steel-reinforced beams, though with a larger deflection (Nanni, *et al.* 1994(a)). These experimental results agreed with theoretical data and lead to the conclusion that hybrid rods may become a viable option for use in reinforced concrete applications.

## 3. Bond characterization

### 3.1. Bond test procedures

To date there is no US standard test available to determine bond strength between concrete and reinforcing bars. The American Society for Testing and Materials (ASTM) has developed a standard concentric pull-out test ("Standard" 1991). This test was originally intended for comparison of different concrete mixtures. The test offers the advantage of simplicity but presents two disadvantages: 1) the concrete surrounding the reinforcing bar tends to split, and 2) the concrete is subjected to compression at the loading face. Criteria for the determination of bond strength using this test may be based on an arbitrary value of the bond slip (at the load-end or at the free-end), or on the ultimate bond strength of the bar (provided that pull-out occurs before yielding of the bar).

To remove compression on the concrete face, a modified version consists of a specimen made of a concrete prism in which two bars are embedded at the opposite ends (Chapman and Shah 1987). The two bars have different embedment lengths so that failure is restricted to the short one. In a number of research works, the specimens used in the pull-out test included confining

reinforcement to prevent splitting of the concrete (Soroushian, *et al.* 1991).

The eccentric pull-out test is thought to be a more realistic representation of what happens in a beam in terms of bond performance, but it does not allow for the formation of diagonal tension cracks common in flexure (Lutz and Gergely 1967).

Other tests such as the modified beam and cantilever beam tests solve some of the stress field discrepancies of the concentric and eccentric pull-out tests. Flexural-type tests offer the advantage of representing the actual situation more closely. In some cases, the beam-end specimens had load applied directly to the reinforcing bar (Johnston and Zia 1982); in other cases, the set-up was that of an inverted simply-supported beam with 4-point load (Treece and Jirsa 1989). In any case, tests can be used not only for the determination of bond strength but also crack width and crack spacing.

## 3.2. FRP-concrete bond studies

Fragmented and inconclusive findings are available from research works in North America. Pull-out tests were performed on glass and carbon FRP strands embedded in cylinders and prisms (Iyer and Anigol 1991). The FRP strands made with 7 twisted small-diameter rods, showed bond strength values comparable to that of conventional steel strands. Pultruded glass and aramid rods with surface deformation (45 degree helical wrap) were used for pull-out tests from concrete cylinders (Pleimann 1991, Challal and Benmokrane 1992, Tao, *et al.* 1992, Larralde and Silva-Rodriguez 1993). Laboratory results indicated an ultimate bond strength lower than for conventional steel reinforcing bars. One theory is that the surface deformations on the FRP bars were less pronounced than the lugs on the steel reinforcing bars and, therefore, had less bearing against the concrete (Larralde and Silva-Rodriguez 1993). Ribbed and sand-coated glass FRP rods were used in pull-out as well as cantilever-type beam specimens for the determination of bond properties (Gangarao and Faza 1991). The conclusion of this study was that for sand-coated FRP bars, development length requirements can be predicted by using Building Code equations for conventional steel reinforcing bars ("Building" 1989). In a study using 27 beam specimens to determine the bond characteristics of ribbed glass FRP rods (Daniali 1990), it was found that only 12 mm bars could develop sufficient bond strength, whereas all bars with larger diameter (19 and 25 mm) failed in bond.

Research in Europe and Japan is based on FRP commercial products developed in those countries. This research indicates that the bond strength of FRP composites depends on several factors, such as the surface pattern of the rod, the ratio of surface area to cross-section of the rods, and the thickness, shear strength and shear modulus of the rod's surface layer ("High-Strength" 1992). For aramid FRP flat strips, it was reported that bond is satisfactory under both static and fatigue conditions (Gerritse 1990). However, it was suggested that in applications where temperature fluctuation occurs, the effect of different coefficients of thermal expansion should be addressed. The research work on bond reported in the Japanese literature is primarily the result of two Ph.D. dissertations (Maruyama 1990 and Tanigaki 1991). Relevant to this study are the results presented in Fig. 2 (Tanigaki 1991). These data were obtained by concentric pull-out tests on FRP rods embedded in concrete cubes (150 mm in side, 34.2 MPa compressive strength) over a length equal to six times the rod diameter. The slip was measured at the free-end. The rod samples are braided aramid FRP rods with no coating (K96=10 mm diameter) and with sand coating (K96S=11 mm and K192S=15.5 mm); braided carbon FRP rods without
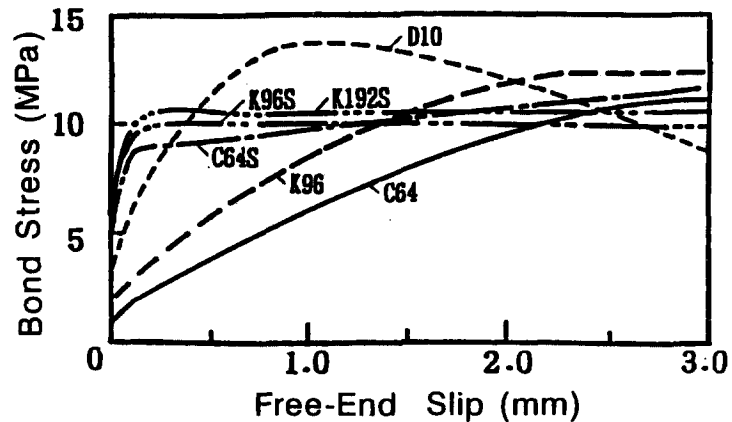
Fig. 2 Bond stress *vs.* free-end slip (Tanigaki 1991).

coating (C64=8 mm) and with sand coating (C64S=9 mm). FRP rods are compared with a deformed steel reinforcing bar (D10=10 mm). Even though the ultimate bond strength of braided FRP rods with no coating is equivalent to that of the steel reinforcing bar, it occurs at a considerably larger level of slip. Using a similar specimen configuration (embedment length constant at 80 mm), Maruyama (1990) used six different FRP rod types and three steel rods. Experimental bond-slip curves led to conclusions similar to those arrived at by Tanigaki. This research also addressed the effect of other variables such as concrete strength and temperature (from +20 to +100°C) showing that high temperature had a very detrimental effect on bond.

## 4. Experimental method and procedure

### 4.1. Specimens

Eleven different types of hybrid rods (coded H1 through H11 as shown in Table 1, Column 1) were used, based on various geometries and types of FRP skins and steel cores. Hybrid rods were custom fabricated. An hybrid rod is schematically represented in Fig. 1. The braided FRP skin was made of either aramid or poly-vinyl alcohol (PVA) type fibers, denoted 'K' and 'V' respectively (Table 1, Column 2), impregnated with epoxy resin. The FRP skin itself varied in thickness, labeled 48, 64, or 96 according to values of three cross-sectional areas (Table 1, Column 3). The cores were either of high strength (SBPR80) or low strength (SR24) steel and had diameters of 9.0, 9.2, or 13.0 mm (Table 1, Column 4). For bookkeeping purposes, each rod was labeled according to type and configuration of FRP, diameter of steel core, and type of steel (e.g., K48/9 mm/SR24). The values of longitudinal strength and rigidity were 1489 MPa and 68.4 GPa for the aramid FRP skin, and 429 MPa and 15 GPa for the PVA FRP skin. The minimum yield points of the two steel cores were 235 MPa (SR24) and 784 MPa (SBPR80).

Table 2 shows a summary of all 39 pull-out tests. Two sets of hybrid rods were tested, 18 in one set, and 14 in the other. For comparison, three no. 5 (16 mm) and four no. 4 (13 mm)

Table 1 Hybrid rods (Types and cross-sectional areas)

| Code | Type of rod* | FRP area $(mm^2)$ | Steel area $(mm^2)$ |
|------|-------------|-------------------|---------------------|
| (1) | (2) | (3) | (4) |
| H1 | K48/9 mm/SR24 | 33 | 63.6 |
| H2 | K64/9 mm/SR24 | 42 | 63.6 |
| H3 | K96/9 mm/SR24 | 65 | 63.6 |
| H4 | K64/9.2 mm/SBPR80 | 42 | 66.5 |
| H5 | K96/9.2 mm/SBPR80 | 65 | 66.5 |
| H6 | K96/13 mm/SR24 | 65 | 132.7 |
| H7 | K96/13 mm/SBRP80 | 65 | 132.7 |
| H8 | V48/9 mm/SR24 | 38 | 63.6 |
| H9 | V64/9 mm/SR24 | 50 | 63.6 |
| H10 | V96/9 mm/SR24 | 75 | 63.6 |
| H11 | V96/9.2 mm/SBRP80 | 75 | 66.5 |

Note: *FRP type and thickness/steel core diameter/steel grade
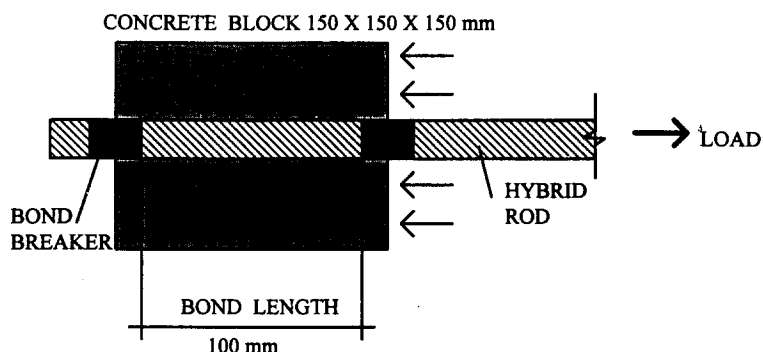


Fig. 3 Specimen characteristics.

deformed steel reinforcing bars (Grade 40 and 60, respectively) were also tested. The coded list of tested specimens is given in Column 1 of Table 2 (e.g., H1-1-a, corresponds to hybrid rod H1, repetition 1, concrete type a). The repetition 1 is always associated with the lower ultimate load test result. Column 2 gives the rod type. Column 3 shows the tensile load at which the core yields, and Column 4 shows the load at which the FRP ruptures (Nanni, et al. 1994). All rods were embedded in identical concrete cubes (150 mm in side). The only variation was that one batch of specimens was tested in concrete with compressive strength of 14.4 MPa (mix a) and the other in concrete of strength 36.2 MPa (mix b) (See Table 2, Column 5). The embedment length in the concrete was controlled and maintained at 100 mm for all specimens by taping off sections of rod before casting in the concrete (see Fig. 3).

## 4.2. Test set-up

Concentric pull-out tests were performed with a universal testing machine. Linear variable differential transformer (LVDT) devices, wired to a data acquisition system, were used to measure

Table 2 Rod tensile properties and pull-out test results

| Code | Type of rod | Tension | | $f'_c$ | Pull-out test | | | | |
|------|-------------|---------|---------|-------|------|--------|----------|------|------|
| | | Yield load (kN) | Ult. load (kN) | (MPa) | Ult. load (kN) | Failure mode | Bond strength (MPa) | Free-end slip (mm) | Load-end slip (mm) |
| (1) | (2) | (3) | (4) | (5) | (6) | (7) | (8) | (9) | (10) |
| H1-1-a | K48/9 mm/SR24 | 25.4 | 68.1 | 14.4 | 15.76 | split | 4.56 | 1.91 | 3.03 |
| H1-2-a | | | | | 16.01 | split | 4.63 | 1.11 | 2.48 |
| H2-1-a | K64/9 mm/SR24 | 26.5 | 81.4 | 14.4 | 15.51 | split | 4.26 | 0.98 | 3.12 |
| H2-2-a | | | | | 19.31 | split | 5.30 | 1.90 | 2.58 |
| H3-1-a | K96/9 mm/SR24 | 29.2 | 115.6 | 14.4 | 17.79 | split | 4.42 | 1.08 | 3.07 |
| H3-2-a | | | | | 19.57 | split | 4.87 | 0.83 | 3.23 |
| H4-1-a | K64/9.2 mm/SBPR80 | 113.2 | 152.1 | 14.4 | 18.05 | split | 4.87 | 1.50 | 2.98 |
| H4-2-a | | | | | 21.35 | split | 5.64 | 0.81 | 3.71 |
| H5-1-a | K96/9.2 mm/SBPR80 | 124.2 | 186.2 | 14.4 | 18.05 | split | 4.45 | 1.29 | 3.57 |
| H5-2-a | | | | | 19.83 | split | 4.89 | 1.30 | 2.84 |
| H6-1-a | K96/13 mm/SR24 | 49.6 | 136.3 | 14.4 | 25.42 | split | 5.09 | 1.15 | 2.34 |
| H7-1-a | K96/13 mm/SBPR80 | 216.9 | 275.7 | 14.4 | 22.88 | split | 4.58 | 0.75 | 2.10 |
| H8-1-a | V48/9 mm/SR24 | 22.6 | 35.3 | 14.4 | 23.89 | y/pull-out | 6.67* | 2.31 | 5.00 |
| H8-2-a | | | | | 24.91 | y/split | 6.95# | 2.98 | 5.23 |
| H9-1-a | V64/9 mm/SR24 | 23.0 | 40.8 | 14.4 | 18.56 | split | 4.92 | 2.01 | 2.53 |
| H9-2-a | | | | | 24.15 | y/pull-out | 6.40* | 2.75 | 4.78 |
| H10-1-a | V96/9 mm/SR24 | 23.5 | 51.3 | 14.4 | 13.98 | split | 3.34 | 0.79 | 1.17 |
| H10-2-a | | | | | 20.08 | split | 4.81 | 1.51 | 3.74 |
| S1-1-a | No. 5 Deformed | 64.2 | 64.2 | 14.4 | 18.81 | split | 3.77 | 0.26 | 0.65 |
| S2-1-a | No. 4 Deformed | 55.7 | 55.7 | 14.4 | 18.05 | split | 4.52 | 0.17 | 1.95 |
| S2-2-a | | | | | 22.62 | pull-out | 5.67 | 0.61 | 1.74 |
| H1-1-b | K48/9 mm/SR24 | 25.4 | 68.1 | 36.2 | 20.00 | pull-out | 5.78 | 2.20 | 5.00 |
| H1-2-b | | | | | 34.79 | y/pull-out | 10.07* | 1.89 | 5.00 |
| H2-1-b | K64/9 mm/SR24 | 26.5 | 81.4 | 36.2 | 28.90 | y/pull-out | 7.93* | 1.20 | 5.00 |
| H3-1-b | K96/9 mm/SR24 | 29.2 | 115.6 | 36.2 | 28.00 | y/pull-out | 6.96* | 1.30 | 5.00 |
| H3-2-b | | | | | 40.00 | y/pull-out | 9.95* | 0.66 | 5.00 |
| H7-1-b | K96/13 mm/SBPR80 | 216.9 | 275.7 | 36.2 | 40.61 | split | 8.13 | 2.09 | 2.23 |
| H7-2-b | | | | | 48.61 | split | 9.73 | 2.45 | 2.75 |
| H8-1-b | V48/9 mm/SR24 | 22.6 | 35.3 | 36.2 | 24.00 | y/pull-out | 6.72* | 1.27 | 5.00 |
| H8-2-b | | | | | 24.07 | y/pull-out | 6.72* | 2.17 | 4.75 |
| H9-1-b | V64/9 mm/SR24 | 23.0 | 51.3 | 36.2 | 27.38 | y/pull-out | .4.74* | 1.60 | 5.00 |
| H10-1-b | V96/9 mm/SR24 | 23.5 | 51.3 | 36.2 | 20.00 | y/pull-out | 4.74* | 1.60 | 5.00 |
| H10-2-b | | | | | 25.00 | y/pull-out | 5.93* | 1.50 | 5.00 |
| H11-1-b | V96/9.2 mm/SBPR80 | 101.0 | 118.1 | 36.2 | 41.52 | split | 9.86 | 3.37 | 3.65 |
| H11-2-b | | | | | 48.59 | split | 11.54 | 4.14 | 4.17 |

Table 2 Continued

| Code | Type of rod | Tension | | $f'_c$ | Pull-out test | | | | |
|---|---|---|---|---|---|---|---|---|---|
| | | Yield load (kN) | Ult. load (kN) | (MPa) | Ult. load (kN) | Failure mode | Bond strength (MPa) | Free-end slip (mm) | Load-end slip (mm) |
| (1) | (2) | (3) | (4) | (5) | (6) | (7) | (8) | (9) | (10) |
| S1-1-b | No. 5 Deformed | 64.2 | 64.2 | 36.2 | 64.10 | y/pull-out | 12.80* | 0.51 | 1.64 |
| S1-2-b | | | | | 64.45 | y/pull-out | 12.90* | 0.18 | 2.60 |
| S2-1-b | No. 4 Deformed | 55.7 | 55.7 | 35.2 | 38.38 | pull-out | 9.62 | 0.75 | 3.18 |
| S2-2-b | | | | | 42.20 | pull-out | 10.58 | 0.72 | 3.10 |

*Indicates yielding before pull-out, #Indicates yielding before split

displacements at three locations: load-end, free-end, and concrete block. A load cell was placed under the concrete block. Measured before each test were two dimensions: 1) the length of rod extending from the block at the free-end, and 2) the distance at the load-end of the LVDT from the block, usually about 350 mm. If the concrete block remained intact at the completion of the test, these measurements were repeated. During testing, the load was applied and gradually increased until the specimen failed, whether by pull-out of the rod, or splitting of the concrete. Either type of failure could be preceded by yielding of the rod core. Measurements of load and deflections at the various points were taken by the data acquisition system every second and saved in a computer file for analysis. The type of failure was recorded.

### 4.3. Assumptions

Pull-out was considered to occur at an arbitrary value of the net load-end slip (5 mm), even though the test was not necessarily ended at this point. The rationale for the choice of 5 mm as the threshold value was in response to the need to allow for yielding of the rod core. When compared to the embedded length, a 5% slip appears to be a sufficiently high upper limit.

## 5. Experimental results

### 5.1. Maximum load and failure type

Columns 6 and 7 of Table 2 show all values of ultimate pull-out load and failure type. In general, hybrid rods embedded in the low-strength concrete failed by concrete splitting, whereas failure by pull-out was observed in the instance of higher-strength concrete. By comparing the values of the recorded pull-out load with the yield point for the rod core, it is possible to determine if yielding occurred prior to failure by splitting or pull-out. For the latter, yielding of the core occurred in all cases but one as shown by "y/" in Table 2, Column 7. This obviously depends on the definition adopted for pull-out failure (i.e., 5 mm net load-end slip).
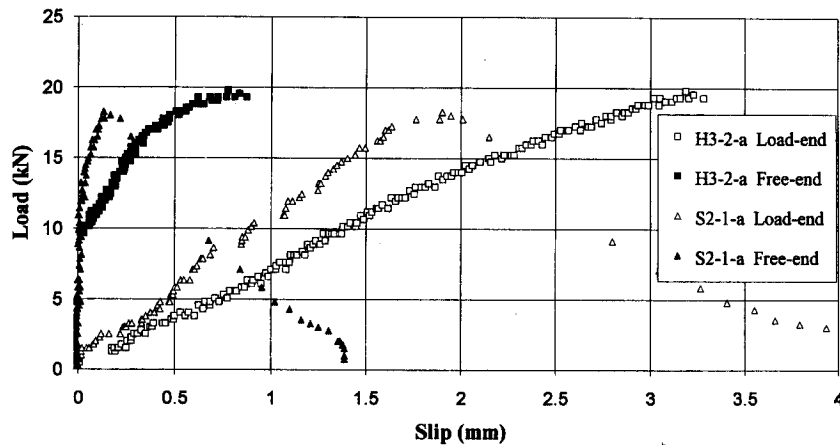
### 5.2. Load-slip diagrams

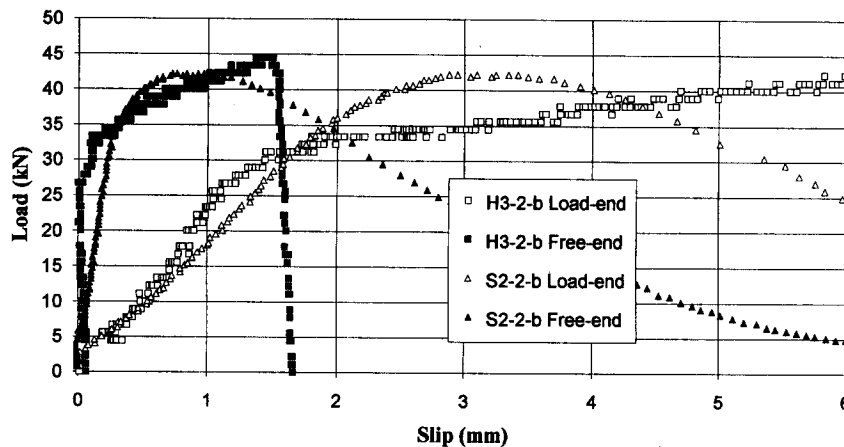Fig. 4 Load-slip diagrams at free-end and load end (14.4 MPa concrete).



Fig. 5 Load-slip diagrams at free-end and load end (36.2 MPa concrete).

Load-slip diagrams were constructed from the raw data. The movement of the concrete block indicated the movement of the entire system. Therefore, this value was subtracted from the load-end and the free-end displacements. Further manipulation of the net load-end displacement was required to account for elastic elongation of the unbonded length (distance of the LVDT from the concrete block plus 25 mm of bond breaker). Subtracting $PL/AE$ (where: $P$=load, $L$= length, $A$=cross sectional area of the rod, $E$=modulus of elasticity of the rod) from the net load-end displacement gave the net load-end slip. As an example of the diagrams that were obtained, Figs. 4 and 5 show the applied load plotted as a function of net free-end and load-end slip for two specimens, respectively. Fig. 4 is relative to specimens H3-2-a and S2-1-a. The total area of hybrid and reference standard reinforcing bar is approximately the same (i.e., 63.6 plus 65 equal to 128.6 mm$^2$, and 129 mm$^2$), and both specimens fail due to splitting of the 14.4 MPa concrete block. The maximum load is also approximately the same (i.e., 19.57 and 18.05 kN). However, the free-end and load-end slip of the hybrid rod at maximum load are
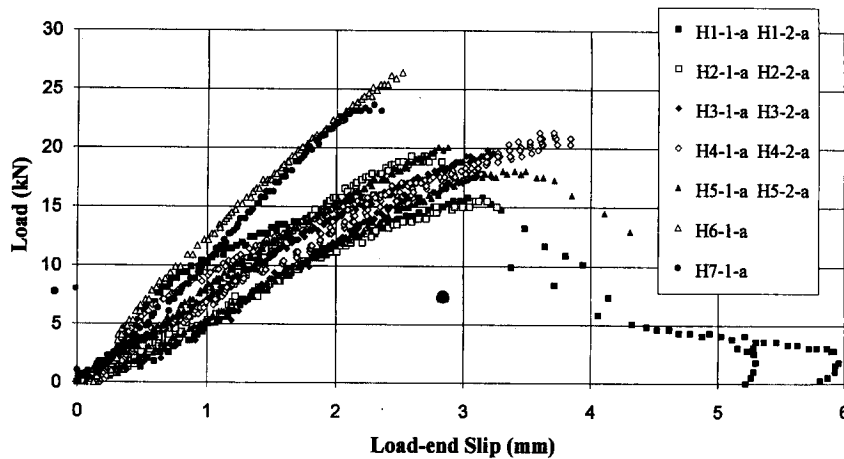
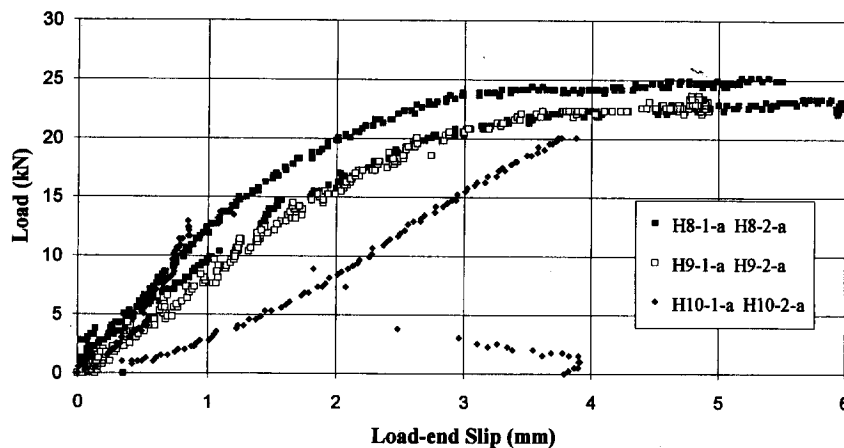Fig. 6 Load *vs.* load-end slip (Aramid FRP-14.4 MPa concrete).



Fig. 7 Load *vs.* load-end slip (PVA FRP-14.4 MPa concrete).

considerably higher than that of the steel reinforcing bar (0.78 and 0.13 mm, and 3.23 and 1.95 mm). Fig. 5 shows the same type of rods when embedded in the stronger 36. 2 MPa concrete (H3-2-b and S2-2-b). Failure is this time by pull-out and the following observations are made: 1) the core of the hybrid rod yields when the load-end slip is approximately 2 mm, and from there on the slope of the load-slip curves (both load-end and free-end) is very flat; 2) maximum load for the steel reinforcing bar occurs at a load-end slip of 3.1 mm followed by a descending branch of the load-slip curves (both load-end and free-end) as concrete is sheared off between the rod lugs; and, 3) Up to approximately 2 mm load-end displacement, there is not a significant difference between the slope of the load-slip curves of hybrid and reference rod.

Figs. 6 to 9 show the load-slip diagrams relative to the load-end for all hybrid rods. Fig. 6 is relative to the aramid FRP hybrid rods embedded in the 14.4 MPa lower strength concrete. All specimens failed by splitting of the concrete (See Table 2, Column 7) at values of load-end slip less than 4 mm. There is a very good consistency of results: all rods with the 9 and 9.2 mm core form one group, and rods with 13 mm core form a second one. There seems
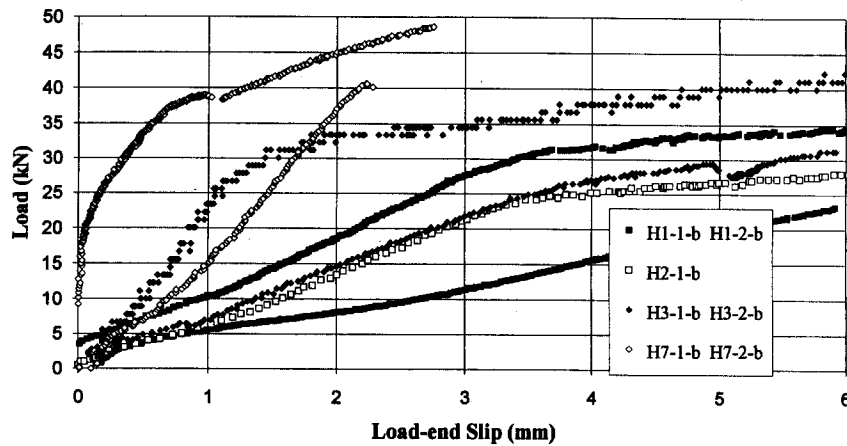
Fig. 8 Load *vs.* load-end slip (Aramid FRP-36.2 MPa concrete).
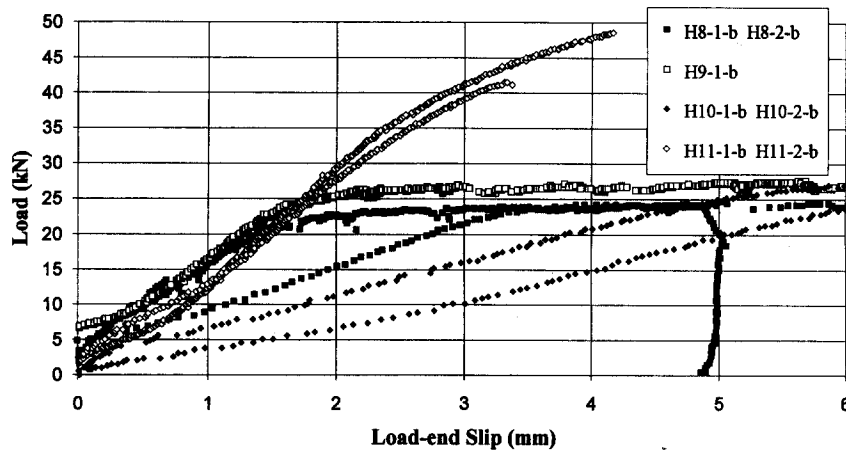


Fig. 9 Load *vs.* load-end slip (PVA FRP-36.2 MPa concrete).

to be little effect due to the FRP skin thickness. Since concrete splits before steel core of any rod can yield, there is no effect due to the grade of the steel core.

Fig. 7 is relative to PVA FRP hybrid rods (all with 9 mm mild steel core) embedded in the lower strength concrete. This time pull-out or concrete splitting failures was observed (Table 2, Column 7), in addition three of the rods with smaller skin thickness (V48 and V64) yielded prior to failure. The bond strength appears to be higher than in the previous case of aramid FRP (compare H1, H2 H3 with H8, H9, H10), but it is accompanied by larger slip. The load-slip diagrams for the two specimens H10 have significantly different slopes. H10-1-a also failed prematurely. It is possible that the scatter among identical specimens be the result of bond mechanism between hybrid rod and concrete. In a steel deformed reinforcing bar, bond is controlled by mechanical interlock, here friction plays the predominant role as the hybrid rod slips without causing damage to the surrounding concrete.

Fig. 8 is a repetition of Fig. 6 for the case of 36.6 MPa concrete strength. With the exception of the 13 mm rods (H7), the mode of failure is pull-out (i.e., net load-end slip larger than 5
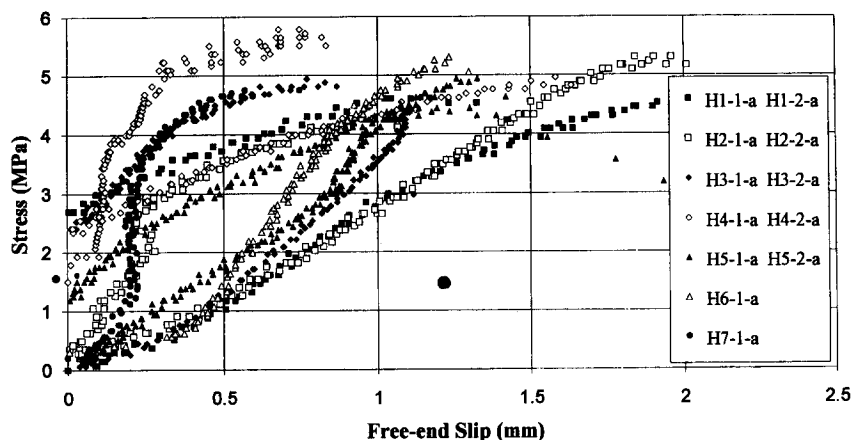
Fig. 10 Bond stress *vs.* free-end slip (Aramid FRP-14.4 MPa concrete).

mm) preceded by steel core yielding. Even though there is some considerable scatter in slope between curves from identical specimens, the bilinear trend with bend-over point at yielding is clear for all the 9 mm core rods. Since the only variable with respect to the case of Fig. 6 is concrete strength, it is shown that increasing concrete strength increases the bond strength by changing the mode of failure from concrete splitting to rod pull-out.

Fig. 9 shows the case of PVA FRP hybrid rods in 36.2 MPa concrete. The observations derived from this figure are: 1) the 9 mm mild core rods yield and fail by pull-out; 2) there is less scatter and the bilinear behavior is evident; 3) specimens with 9.2 mm high-strength core rods (H11) fail by concrete splitting; and 4) the aramid FRP rods (H1, H2, H3) tend to exhibit higher ultimate loads than the PVA FRP rods (H8, H9, H10) because, after yielding of the core, the aramid skin can provide a significant contribution to load carrying capacity.

Test results obtained for hybrid rods can be compared with those obtained with standard deformed reinforcing bars nos. 4 and 5. The no. 4 reinforcing bar is used for comparison with the hybrid rods having cores of 9 and 9.2 mm, whereas the no. 5 reinforcing bar is compared to the 13 mm core hybrid rods. By considering the data shown in Table 2 (Columns 6, 9, and 10) some general observations can be drawn. Ultimate loads for the batch of 14.4 MPa concrete showed ranges of 18-23 kN for the steel reinforcing bars and 15-25 kN for the hybrid rods. Steel reinforcing bars in the tests with the 36.2 MPa concrete averaged ultimate loads in the range 38-64 kN, whereas the hybrid rods ranged anywhere from 20-49 kN.

### 5.3. Effective bond strength

The ultimate load is converted to ultimate bond strength, and is given in Column 8 of Table 2, together with the corresponding ultimate free- and load-end slip values (Columns 9 and 10). In terms of bond strength, the hybrid rods proved comparable to steel. For the tests with the 14.4 MPa concrete, the aramid FRP rods exhibited bond strengths in the range of 4.3-5.6 MPa, the PVA FRP rods 3.3-6.9 MPa, and the steel reinforcing bars showed strengths from 3.8-5.7 MPa. The difference, however, was in the fact that the hybrid rods slipped considerably more than the steel reinforcing bars, with free-end displacements of 0.7 -3.0 mm as opposed to 0.2-

0.6 mm for the steel. For the tests with the 36.2 MPa concrete, the strength ranges are 5.8-10.1 MPa for the aramid FRP rods, 4.7-11.5 MPa for the PVA FRP rods, and 9.6-12.9 MPa for the steel. The hybrid rods seem to be less effective than steel reinforcing bars as the concrete strength increases because excessive slip becomes the controlling factor rather than concrete splitting. For 36.2 MPa concrete strength, the free-end slip for the hybrid rods tends to be three to five times the free-end slip of steel reinforcing bars.

Fig. 10 shows a plot of the nominal bond stress as a function of free-end slip for all aramid FRP rods with 14.4 MPa concrete strength. The results indicate that bond strength is not highly dependent on FRP skin thickness, whereas the ultimate slip seems to be inversely proportional to skin thickness. These results can be compared to those presented in Fig. 2 relative to non-hybrid FRP rods of equivalent manufacturing. For example, one can observe that the bond stress of the K96 rod (i.e., braided aramid FRP, 10 mm diameter, 34.2 MPa concrete) is 5.8 MPa when the free-end slip is 0.5 mm. From Figs. 4 and 5, one can see that the bond stress for the same free-end slip is 4.5 and 9.3 MPa for hybrid rod K96/9 mm/SR24 embedded in 14.4 and 36.2 MPa concrete, respectively.

## 6. Conclusions

FRP skin plus steel core hybrid rods may be of interest in the construction industry for application in reinforced (prestressed and not) concrete members. The bond behavior of these new reinforcing elements with concrete was experimentally established in this study. This project examined the performance of hybrid rods with different braided FRP skins and steel cores using the concentric pull-out test. Within the limitations of the sample size and the nature of the test, it was possible to make the following observations:

(1) the overall bond strength of hybrid rods is not significantly lower than that of deformed steel reinforcing bars of similar diameter

(2) the free-end and load-end slip of hybrid rods at given values of pull-out load is significantly higher than that of standard deformed steel reinforcing bars of similar diameter

(3) the higher the concrete strength, the higher the bond strength of hybrid rods as the failure mode changes from concrete splitting to rod pull-out

(4) there is some significant scatter among load-slip diagrams of identical specimens. This may be caused by the predominance of the friction mechanism over mechanical interlocking From an experimental point of view, one of the pressing needs is to increase the data base to offer statistical significance to the observations on bond behavior as listed above.

From a practical stand point, it may be more important to establish the performance of hybrid rods in terms of improved durability with respect to un-coated and epoxy-coated steel reinforcement. Satisfactory results would strongly affect the economical viability of the new reinforcing system.

## Acknowledgements

## References

ACI Committee 318, (1989), "Building code requirements for reinforced concrete and commentary", American Concrete Institute, Detroit, MI, 347.

ASTM C 24-91a, (1991), "Standard test method for comparing concretes on the basis of the bond developed with reinforcing steel", American Society for Testing and Materials, Philadelphia, PA, 5.

CEB Task Group IV, (1982), "Bond action and bond behavior of reinforcement-state of the art report", Bulletin d' Information No. 151, Comite Euro-International du Beton (CEB), Paris, France, April 1982, 153.

Challal, O. and Benmokrane, B. (1993), "Pull-out and bond of glass fiber rods embedded in concrete and cement grout", *RILEM Materials and Structures*, **26**, 167-175.

Chapman, R.A. and Shah, S.P. (1987), "Early-age bond strength in reinforced concrete", *ACI Materials Journal*, **84**(6), 501-510.

Daniali, S. (1990). "Bond strength of fiber reinforced plastic bars in concrete", *Proc., I Materials Eng. Congress*, Denver, CO, American Society of Civil Engineers, New York, NY, 1182-1191.

FIP Commission on Prestressing Materials and Systems-Working Group on FRP, (1992), "High-strength fiber composite tensile elements for structural concrete", Final Version of the State-of-the-Art Report, Federation Internationale de la Precontrainte, London, UK, 140.

Gangarao, H.V.S. and Faza, S.S. (1991), "Bending and bond behavior and design of concrete beams reinforced with FRP reinforcing bars", *FHWA-WV DOH Report*, Dept. of Civil Eng., Univ. of West Virginia, Morgantown, WV, 200.

Gerritse, A. (1990). "Applications and design criteria for aramid fibrous tensile elements", *Proc., Composite Materials in Building: State-of-the-Art, Research, and Prospects*, Consiglio Nazionale Ricerche, Milan, Italy, 317-333.

Iyer, S.L. and Anigol M. (1991), "Testing and evaluating fiberglass, graphite and steel prestressing cables for pretensioned beams", *Proc., Advanced Composites Materials in Civil Engineering Structures*, ASCE Specialty Conference, Las Vegas, NE, American Society of Civil Engineers, New York, NY, 44-56.

Johnston, D. S. and Zia, P. (1982), "Bond characteristics of epoxy coated reinforcing bars", *Report No. FHWA/NC/82-002*, Department of Civil Engineering, North Carolina State University, Raleigh, NC, 163.

Larralde, J. and Silva-Rodriguez, R. (1993), "Bond and slip of FRP reinforcing bars in concrete", *Journal of Materials in Civil Engineering, ASCE*, **5**(1), 30-40.

Lutz, L.A. and Gergely, P. (1967), "Mechanics of bond and slip of deformed bars in concrete", *ACI Journal, Proceedings* **64**(11), 711-721.

Maruyama, T. (1990), "Experimental research into the use of carbon fiber-reinforced-plastic rods for concrete reinforcement", Doctoral Thesis, University of Tokyo, Tokyo, Japan, 207.

Nanni, A., Henneke, M.J. and Okamoto, T. (1994), "Tensile properties of hybrid rods for concrete reinforcement", *Construction and Building Materials*, **8**(1), 27-34.

Nanni, A., Henneke, M.J. and Okamoto, T. (1994a), "Behavior of concrete beams with hybrid reinforcement", *Construction and Building Materials*, **8**(2), 89-95.

Nanni, A., Okamoto, T., Tanigaki, T. and Henneke, M. (1992), "Hybrid (FRP + Steel) reinforcement for concrete structures", *Proc., ASCE Materials Engineering Congress*, Atlanta, GA, American Society of Civil Engineers, New York, NY., 655-663.

Nanni, A. and Liu, J. (1997), "Modeling of bond behavior of hybrid rods for concrete reinforcement", *Structural Engineering and Mechanics, An, Int'l Journal*, **5**(4), 355-368.

Pleimann, L.G. (1991), "Strength, modulus of elasticity, and bond of deformed FRP rods", *Proc., Advanced Composites Materials in Civil Engineering Structures, ASCE Specialty Conference*, Las Vegas, NE, American Society of Civil Engineers, New York, NY, 99-110.

Soroushian, P., Choi, K.B., Park, G.H. and Aslani, F. (1991), "Bond of deformed bars to concrete: effects of confinement and strength of concrete", *ACI Materials J.*, **88**(3), 227-232.

Tanigaki, M. (1991), "Flexural behavior of concrete beams reinforced with high strength fiber rods", Doctoral Thesis, Waseda University, Tokyo, Japan, 124.

Tao, S., Ehsani, M.R. and Saadatmanesh, H. (1992), "Bond strength of straight GFRP reinforcing bars",

*Proc., ASCE Materials Engineering Congress, Atlanta,* GA, American Society of Civil Engineers, New York, NY., 598-605.

Treece, R.A. and Jirsa, J.O. (1989), "Bond strength of epoxy-coated reinforcing bars", *ACI Materials Journal,* **86**(2), 167-174.